THEMIS observations of a secondary magnetic island within the Hall electromagnetic field region at the magnetopause

W.-L. Teh,[1] S. Eriksson,[1] B. U. Ö. Sonnerup,[1,2] R. Ergun,[1] V. Angelopoulos,[3] K.-H. Glassmeier,[4] J. P. McFadden,[5] and J. W. Bonnell[5]

Received 20 August 2010; revised 16 September 2010; accepted 21 September 2010; published 9 November 2010.

[1] We present THEMIS observations of a small-scale secondary magnetic island within the Hall electromagnetic field region at the dayside magnetopause. The reconnecting magnetic fields are nearly symmetric and anti-parallel, whereas the ion plasma density is ~8 times higher in the magnetosheath than in the magnetosphere. In the event, the Hall magnetic and electric fields are asymmetric and stronger on the magnetospheric side of the magnetopause. The small-scale magnetic island was immersed in the out-of-plane Hall magnetic field on the magnetosheath side. We derive a map of the cross section of the magnetic island by use of magnetohydrostatic Grad-Shafranov reconstruction under the force-free assumption. The reconstruction shows a right-handed magnetic island with a length of ~200 km and a width of ~100 km. **Citation:** Teh, W.-L., S. Eriksson, B. U. Ö. Sonnerup, R. Ergun, V. Angelopoulos, K.-H. Glassmeier, J. P. McFadden, and J. W. Bonnell (2010), THEMIS observations of a secondary magnetic island within the Hall electromagnetic field region at the magnetopause, *Geophys. Res. Lett.*, *37*, L21102, doi:10.1029/2010GL045056.

1. Introduction

[2] Magnetic reconnection is an important energy-conversion mechanism in the space plasma environment, converting magnetic field energy into plasma kinetic and thermal energy. The term $\mathbf{j} \times \mathbf{B}/ne$ in Ohm's law, which describes the Hall effect, is a consequence of decoupling of the ion and electron motions that occur when the characteristic scale length becomes comparable to the ion inertial length. Figure 1 shows a schematic of the Hall electromagnetic field configuration around the reconnection site for symmetric anti-parallel field merging at the magnetopause. One of the characteristic signatures of the Hall effect around the reconnection site is an out-of plane, quadrupolar magnetic field pattern, B_H, which is generated by Hall current loops, J_H, resulting from the relative motion of ions and electrons in the inflow toward the reconnection site [*Sonnerup*, 1979; *Terasawa*, 1983]. Another Hall signature is the bipolar electric field, E_H, that points toward the current layer on both sides due to the charge separation of ions and electrons. In the past several years, a substantial amount of observational evidence of Hall signatures in the Earth's magnetosphere has been documented at the magnetopause [*Mozer et al.*, 2002; *Vaivads et al.*, 2004; *Mozer et al.*, 2008], in the magnetosheath [*Phan et al.*, 2007], and also in the magnetotail [*Øieroset et al.*, 2001; *Runov et al.*, 2003; *Borg et al.*, 2005; *Eastwood et al.*, 2007].

[3] Simulations of magnetic reconnection show that secondary magnetic islands can be generated in anti-parallel merging [e.g., *Karimabadi et al.*, 2005; *Daughton et al.*, 2006; *Fujimoto*, 2006; *Klimas et al.*, 2008] as well as in component merging [e.g., *Drake et al.*, 2006]. Understanding the conditions for the formation of the secondary islands has been an important issue in reconnection physics. Recently, *Eastwood et al.* [2007] reported Cluster observations of a secondary magnetic island near a reconnection site in the magnetotail, where Hall electromagnetic fields were also observed. This finding suggests that secondary magnetic islands can be formed in the presence of small reconnection guide field.

[4] In the present paper, we show THEMIS [*Sibeck and Angelopoulos*, 2008] observations of a secondary magnetic island within the asymmetric Hall electromagnetic field of a nearly anti-parallel reconnection event at the dayside magnetopause. We derive the two-dimensional (2D) magnetic field configuration map of the island using magnetohydrostatic Grad-Shafranov (GS) reconstruction [e.g., *Sonnerup and Guo*, 1996; *Hau and Sonnerup*, 1999] for the special case of force-free conditions, i.e., when the gradient of the plasma pressure is neglected [*Hu and Dasgupta*, 2005]. A possible explanation for the asymmetric Hall magnetic field is also discussed.

2. Observations

[5] Our event was encountered by the probe TH-E at the dayside magnetopause at (10.3, 4.5, −2.8) R_E (GSE) on August 6, 2008. Figures 2a–2f show the fields and plasma measurements in the current sheet coordinate system (LMN) for the interval 21:13:35–21:14:55 UT. To simplify the analysis, the vector components are expressed in the Despun, Sun-pointing, L-vector (DSL) system throughout the paper, which is within 8 degrees of the GSE system. Note that in the DSL system the spin-plane is in the $x_{DSL} - y_{DSL}$ plane and the z_{DSL} axis is the spin axis (due approximately north). In Figures 2a–2c, the black (red) curve represents the

[1]Laboratory for Atmospheric and Space Physics, University of Colorado at Boulder, Boulder, Colorado, USA.
[2]Thayer School of Engineering, Dartmouth College, Hanover, New Hampshire, USA.
[3]IGPP, University of California, Los Angeles, California, USA.
[4]Institute for Geophysics and Extraterrestrial Physics, Technical University of Braunschweig, Braunschweig, Germany.
[5]Space Science Laboratory, University of California, Berkeley, California, USA.

0094-8276/10/2010GL045056

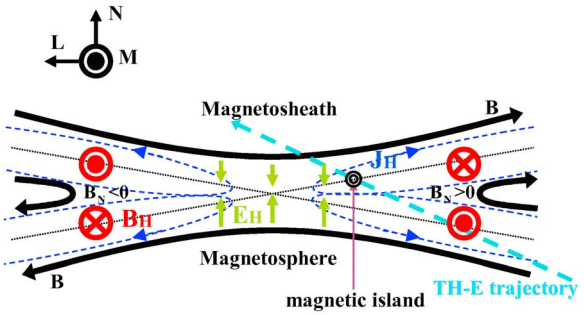

Figure 1. Schematic of Hall electromagnetic field configuration for symmetric anti-parallel field merging at the dayside magnetopause. The LMN coordinates denote the current sheet coordinates. B_H is the out-of-plane quadrupolar Hall magnetic field (red symbols) generated by the Hall currents J_H (blue dashed lines) resulting from the relative motion of ions and electrons in the inflow toward the reconnection site. E_H is the bipolar Hall electric field (green arrows) pointing toward the current sheet. Note that the lengths of the E_H vectors are different on the two sides to indicate the asymmetry of the density across the current sheet. The magnetic island was seen by TH-E within the Hall magnetic field on the magnetosheath side during the reconnection event.

magnetic field (electric field) data. The magnetic and electric field data were obtained from the fast survey observations of the FGM instrument [*Auster et al.*, 2008] and the EFI instrument [*Bonnell et al.*, 2008], with a time resolution of 0.25 sec and 0.125 sec, respectively. Note that the spin-plane electric fields are calibrated by the cross-calibration process [see *Bonnell et al.*, 2008, p. 333]. The spin-axis component of the electric field is derived using the $\mathbf{E} \cdot \mathbf{B} = 0$ assumption, which is less reliable when the magnetic field is close to the spacecraft spin-plane because the spin-axis electric field is then amplified by the small spin-axis magnetic field. For this reason, there are erroneous electric field spikes in Figures 2a–2c near the green dashed line where the field component B_L reverses sign. The spin-resolution (3 sec) ion plasma measurements were obtained from the ESA instrument [*McFadden et al.*, 2008]. The LMN axes in DSL are L = (0.283, −0.340, 0.897) (northward), M = (−0.550, −0.824, −0.139) (dawnward), and N = (0.786, −0.454, −0.420) (sunward), based on the results from minimum variance analysis of the magnetic field (MVAB) in the interval 21:13:35 – 21:14:55 UT [*Sonnerup and Scheible*, 1998]. Given the post-noon spacecraft location, the dawnward orientation of the *N* vector is unusual but, even though the ratio between the intermediate to minimum eigenvalues is ~2.6, the orientation

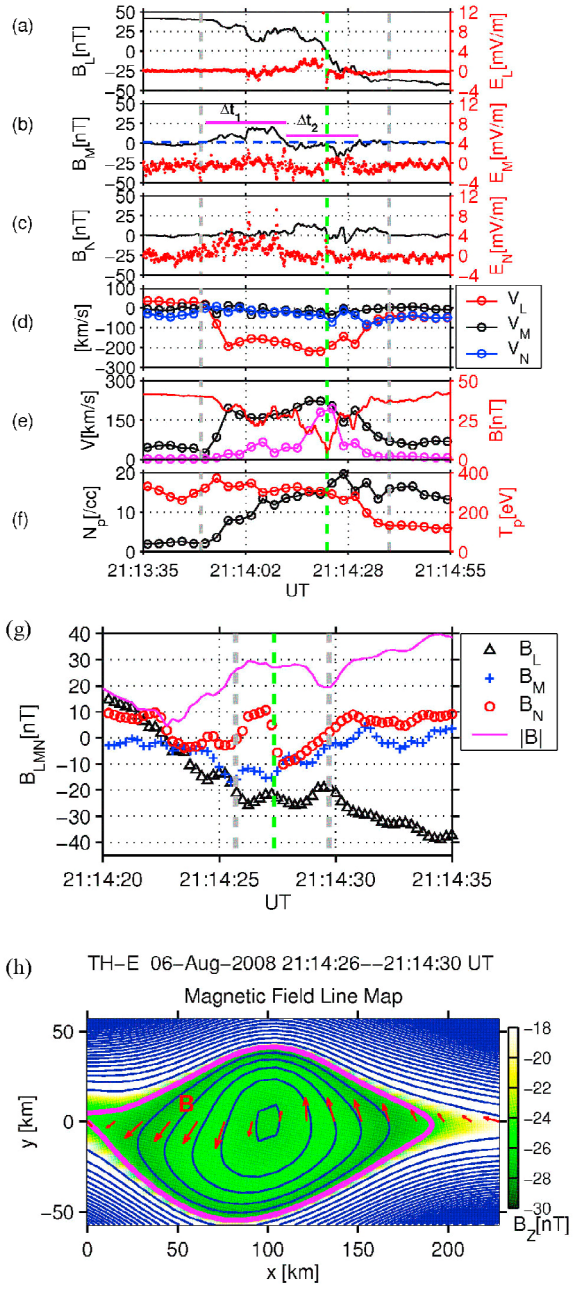

Figure 2. (a–f) TH-E measurements of a reconnection event at the dayside magnetopause on August 6, 2008. The time resolutions for the magnetic field, the electric field, and the plasma data are 0.25 sec, 0.125 sec, and 3 sec, respectively. Vectors are displayed in the current sheet coordinates (LMN). The electric field data are evaluated in the X-line frame (see text). In Figure 2e, the magenta line is the plasma beta (multiplied by 20) and its *y*-axis is to the right. The green dashed line denotes the location where the B_L field component reverses sign. The grey dashed lines mark the start and end of the reconnection exhaust region. In Figure 2b, the horizontal blue dashed line denotes the estimated reconnection guide field of 1.6 nT, and the magenta bar indicates the duration of the Hall magnetic field, where Δt_1 = 21.0 sec and Δt_2 = 18.8 sec. (g) Close-up plot of the magnetic field of the bipolar signature in LMN coordinates. The green line denotes the center of the island. The bipolar signature is enclosed by the two dashed grey lines. (h) TH-E reconstruction map of the magnetic field lines of the island with the axial field B_z in color, using the magneto-hydrostatic reconstruction technique for the force-free condition. The reconstruction axes are: $\hat{\mathbf{x}}$ = (0.200, 0.655, 0.729), $\hat{\mathbf{y}}$ = (−0.980, 0.140, 0.144), and $\hat{\mathbf{z}}$ = (−0.008, −0.743, 0.669), in DSL. The measured transverse magnetic fields are shown by the red arrows at $y = 0$. The positive *y* direction is toward the Earth.

remains the same within ~5° under modest changes of the length and center of the data interval, and in particular the normal field component B_N remains robustly positive. The unusual N direction appears to be the result of magnetic structures in the early part of the event; if these are eliminated, N vector comes close to the nominal magnetopause direction, while B_N still remains positive. In what follows, we will use the LMN system from MVAB.

[6] TH-E experienced a crossing of the magnetopause from the magnetosphere ($B_L > 0$, low density) to the magnetosheath ($B_L < 0$, high density), during which a southward-directed reconnection jet V_L was observed (red curve in Figure 2d). In the event, the reconnecting magnetic field component B_L was nearly the same in magnitude and anti-parallel with a magnetic shear angle of ~178 degrees across the magnetopause, indicating a small reconnection guide field; the ion density in the magnetosheath was ~8 times that in the magnetosphere. The interval enclosed by the two grey dashed lines in Figures 2a–2f denotes the start and end of the accelerated flow event, which is identified as the reconnection exhaust, where the field magnitude at the peak speed of the plasma jet has decreased to 20 nT which is ~48% of the field magnitude (~42 nT) outside the exhaust.

[7] The electric field data in Figures 2a–2c are evaluated in the X-line frame. The estimated X-line frame velocity in DSL is (−47, 50, −61) km/s (tailward and southward), which is −85 km/s along the L direction, −9 km/s along the M direction, and −34 km/s along the N direction. Note that the speeds along the M and N directions are the average speed of V_M and V_N (shown in Figure 2d), respectively, in the interval 21:13:35–21:14:55 UT; the X-line speed along the L direction will be explained below. The peak speed of the ion plasma jet V_L is 219 km/s in the spacecraft frame and 134 km/s in the X-line frame. In the latter frame, the reconnection jet is at ~57% of the Alfvén speed in the magnetosheath ($V_{A,sh}$ = 237 km/s, based on density = 15 cm^{-3} and $B_L \simeq 42$ nT), in reasonable agreement with simulation result by *Karimabadi et al.* [2007], where the reconnection jet was at ~40% of $V_{A,sh}$. In Figure 2b, the measured tangential electric field E_M, transformed to the X-line frame, is −0.53 mV/m on average over the interval 21:13:35 – 21:14:55 UT, which is consistent with the steady-state reconnection electric field, $V_{inflow,sh}B_L \simeq -0.53$ mV/m, with the magnetosheath inflow speed in the X-line frame $V_{inflow,sh} \simeq$ 12.7 km/s and B_L = 42 nT on the magnetosheath side of the event at 21:14:55 UT. The speed of the X-line frame along the $-L$ direction was determined by requiring agreement of E_M in the X-line frame with $V_{inflow,sh}B_L$. The dimensionless reconnection rate $R_X = V_{inflow,sh}/V_{A,sh} = 0.05$, which is approximately consistent with the ratio of average normal magnetic field of +2.6 nT to anti-parallel magnetic field of 42 nT. The positive sign of the average normal magnetic field agrees with the observation that TH-E passed through the southward-directed reconnection jet, as shown in Figure 1. From the magnetopause speed along the normal, v_{mp} = −34 km/s, and the reconnection rate R_X, we can estimate the distance from the spacecraft to the X-point as $(v_{mp}\Delta t)/R_X \simeq$ 5644 km, where Δt = 8.3 sec is the duration between the point where $B_L = 0$ and the end time of the Δt_2 interval in Figure 2b.

[8] As shown by the blue dashed line in Figure 2b, the average guide field is about 1.6 nT or 4% of the reconnecting field B_L. Figure 2b also shows that there are two peaks in the out-of-plane magnetic field component B_M, where the positive (negative) peak is on the magnetospheric (magnetosheath) side of the magnetopause, which is consistent with the predicted quadrupolar Hall magnetic field B_H for the southward-directed reconnection jet, as shown in Figure 1. The peak and duration of the Hall magnetic field are (+19.8 nT, Δt_1 = 21.0 sec) and (−18.6 nT, Δt_2 = 18.8 sec), respectively, for the magnetospheric and magnetosheath sides. Note that the peak values are relative to the average guide field of 1.6 nT and the difference between the two peaks is 1.2 nT, which is ~75% of the reconnection guide field. This indicates that the Hall magnetic field is asymmetric and slightly wider and stronger on the magnetospheric side than on the magnetosheath side. The asymmetric feature is unusual and opposite to the conventional view that the stronger Hall magnetic field should be on the side of higher plasma density [e.g., *Karimabadi et al.*, 1999; *Nakamura and Scholer*, 2000]. In the X-line frame, the normal electric field E_N stays positive within the first lobe of the quadrupolar Hall magnetic field and then turns negative on the second one, as shown in Figure 2c. This pattern is consistent with the predicted Hall electric field $E_H = \hat{\mathbf{N}} \cdot (\mathbf{j} \times \mathbf{B})/ne$ pointing toward the magnetopause current layer on both sides, as shown in Figure 1. Also, the Hall electric field is stronger on the magnetospheric side, where the plasma density is lower, than on the magnetosheath side. The reason is that the Hall electric field is inversely proportional to the plasma density, i.e., $E_H \propto 1/n$, where n is the plasma density.

[9] In addition to the presence of the Hall electromagnetic fields, a small-scale magnetic island was observed during the event. The island was characterized by a strong bipolar positive-then-negative signature of the B_N field component (see Figure 2c) in the region of the Hall magnetic field (in Figure 2b) on the magnetosheath side. Figure 2g shows a close-up view of the bipolar signature, in LMN coordinates. Note that (1) the island is immersed within the Hall fields associated with the ion diffusion region; (2) the magnetic field strength slightly decreases at the center of the island (at the green dashed line in Figure 2g).

3. Reconstruction Results

[10] We employ magnetohydrostatic GS reconstruction [e.g., *Hau and Sonnerup*, 1999; *Sonnerup et al.*, 2004; *Hu and Dasgupta*, 2005; *Hasegawa et al.*, 2006; *Teh and Hau*, 2007] to derive the properties and shape of the magnetic island under the assumptions that its structure is steady-state and two dimensional. The cross-sectional map is constructed using spacecraft data as spatial initial values for the integration of the GS equation. Because of the lack of high-resolution (0.25 sec) plasma measurements, only magnetic field data are used for the reconstruction, which requires the assumption of force-free conditions, i.e., $\mathbf{j} \times \mathbf{B} = 0$. Although this condition is not appropriate in the ion diffusion region as a whole, it may be acceptable within the small magnetic island. The reconstruction is performed in the plane perpendicular to the axis of the island (z direction, positive along the guide field direction) with $+x$-axis along the projection of the spacecraft trajectory on that plane and the y-axis completing an orthogonal system (positive towards Earth). Figure 2h shows the resulting cross section of the magnetic island, with the axial magnetic field B_z in color and

reconstructed in its deHoffmann-Teller (HT) frame [e.g., *Khrabrov and Sonnerup*, 1998]. Using plasma and field data in the interval 21:14:25–21:15:00 UT, the HT frame velocity $\mathbf{V}_{HT}$ is (−82, 80, −133) km/s (tailward and southward), with correlation coefficient of 0.94 between the components of the convection electric field $-\mathbf{V} \times \mathbf{B}$ and the corresponding components of $-\mathbf{V}_{HT} \times \mathbf{B}$. In the X-line frame, the island moves faster than the surrounding plasma, by ~23 km/s. The axis of the island, $\hat{\mathbf{z}}$ = (−0.008, −0.743, 0.669) (dawnward and northward), was chosen such that the axial field B_z remains approximately the same, when the same magnetic field line is encountered at the inbound and the outbound crossing of the island. The reconstruction produces an eye-like island structure with a size of 100 km (width) × 200 km (length) (~1.5 L_i × 3.0 L_i), where the ion inertial length L_i = 59 km is based on a proton density of 15 cm^{-3}. We see that (1) the magnetic island has right-handed helicity as indicated by the measured transverse magnetic field arrows at $y = 0$ in Figure 2h; (2) the island structure enclosed by the magenta line is immersed in the ambient field B_z that originates from the out-of-plane Hall magnetic field on the magnetosheath side.

4. Summary and Discussion

[11] We have presented TH-E observations of a small-scale secondary magnetic island within the ion diffusion region at the dayside magnetopause. The reconnection event occurred for nearly symmetric and anti-parallel magnetic fields and a plasma density ratio of ~8 across the magnetopause. The observed Hall magnetic field pattern was consistent with the southward-directed reconnection jet. The observed Hall electric field was asymmetric and stronger on the magnetospheric side of the magnetopause and directed toward the current sheet, as expected. The observations and the force-free reconstruction in Figure 2h show that the secondary magnetic island was immersed in the ambient field that originates from the out-of-plane Hall magnetic field on the magnetosheath side. The reconstruction produces a right-handed magnetic island structure with a size of about 100 km × 200 km. Note that for a magnetic flux rope with a typical size of 1 R_E × 1 R_E, the island is ~64 times smaller in width and ~32 times smaller in length. In the absence of plasma observations at the needed resolution of 0.25 sec, we have tested the robustness of the reconstructed field map by also doing reconstructions with various assumed plasma pressure profiles, which had higher pressure at the center of the island with exponential decrease away from the center. These experiments indicate that the island width will shrink with increasing plasma pressure at the island center. The observations show that the island is not centered within the exhaust. This may be the result from an angle of ~8 degrees between the direction of motion of the X-line and that of the island. However, since the estimated X-line is ~5644 km (~96 L_i) away from the spacecraft, we cannot exclude the possibility that the island was formed elsewhere and was not related to this particular X-line. From single-spacecraft observations, we are also unable to tell whether such small islands are forming repeatedly [e.g., *Karimabadi et al.*, 2005].

[12] The asymmetric Hall magnetic field is unusual in that the stronger field is on the magnetospheric side of the magnetopause. One would rather expect a stronger Hall magnetic field on the side of higher plasma density. A possible explanation is that this asymmetric Hall magnetic field is a consequence of spatial-temporal effects during the observations, such as time evolution of the Hall features and geometric considerations as the spacecraft traversed the diffusion region. For a symmetric configuration, each lobe of the quadrupolar Hall magnetic field has the same spatial variation such that it peaks at some distance along the separatrix from the X-point and then decreases away from its peak. The observed Hall magnetic field strength could thus be asymmetric simply as a result of an inclined spacecraft trajectory (see Figure 1) through the current sheet: the spacecraft may spend longer time close to the strong Hall magnetic field on the magnetospheric side than on the magnetosheath side. This conjecture is consistent with the calculated inclination angle which is ~$\tan^{-1}(V_N/V_L)$ = 22°, using velocities in the X-line frame. The observations (see Figures 2b and 2c) also show a slightly wider region of the Hall electromagnetic field on the magnetospheric side than on the magnetosheath side of the magnetopause. Additionally, the observation shows that the Hall magnetic field on the magnetosheath side in fact extended into the magnetospheric side of the current sheet. This feature is consistent with reconnection simulations in an asymmetric reconnection configuration [e.g., *Karimabadi et al.*, 1999; *Nakamura and Scholer*, 2000].

[13] Figure S1 of the auxiliary material[1] shows the electric field structure inside the magnetic island in LMN coordinates and in the spacecraft frame; it is similar to the result shown in Figure 11 of the work by *Eastwood et al.* [2007]. We find that (1) the transverse electric field E_M^{sc} reverses sign near the center of the island and that (2) there is a negative/positive/negative tripolar signature in the E_L^{sc} field component. These findings are consistent with the results reported by *Eastwood et al.* [2007] for a secondary magnetic island, observed within the ion diffusion region in the magnetotail. However, in contrast to the magnetotail event, TH-E did not observe a strong enhancement of the total magnetic field strength at the center of the island but instead a slight field decrease. Both reconnection events demonstrate that secondary magnetic islands can be generated within the ion diffusion region when the reconnection guide field is small.

[14] **Acknowledgments.** WLT thanks W.-L. Liu for providing TH-E electric field data. This work was supported by NASA grant NAS5-02099 to LASP at the University of Colorado at Boulder.

[1] Auxiliary materials are available in the HTML. doi:10.1029/2010GL045056.

References

Auster, H.-U., et al. (2008), The THEMIS Fluxgate Magnetometer, *Space Sci. Rev.*, *141*, 235–264, doi:10.1007/s11214-008-9365-9.

Bonnell, J. W., et al. (2008), The Electric Field Instrument (EFI) for THEMIS, *Space Sci. Rev.*, *141*, 303–341, doi:10.1007/s11214-008-9469-2.

Borg, A. L., M. Øieroset, T. D. Phan, F. S. Mozer, A. Pedersen, C. Mouikis, J. P. McFadden, C. Twitty, A. Balogh, and H. Rème (2005), Cluster encounter of a magnetic reconnection diffusion region in the near-Earth magnetotail on September 19, 2003, *Geophys. Res. Lett.*, *32*, L19105, doi:10.1029/2005GL023794.

Daughton, W., J. D. Scudder, and H. Karimabadi (2006), Fully kinetic simulations of undriven magnetic reconnection with open boundary conditions, *Phys. Plasmas*, *13*, 072101, doi:10.1063/1.2218817.

Drake, J. F., M. Swisdak, K. M. Schoeffler, B. N. Rogers, and S. Kobayashi (2006), Formation of secondary islands during magnetic reconnection, *Geophys. Res. Lett.*, *33*, L13105, doi:10.1029/2006GL025957.

Eastwood, J. P., T.-D. Phan, F. S. Mozer, M. A. Shay, M. Fujimoto, A. Retinò, M. Hesse, A. Balogh, E. A. Lucek, and I. Dandouras (2007), Multi-point observations of the Hall electromagnetic field and secondary island formation during magnetic reconnection, *J. Geophys. Res.*, *112*, A06235, doi:10.1029/2006JA012158.

Fujimoto, K. (2006), Time evolution of the electron diffusion region and the reconnection rate in fully kinetic and large system, *Phys. Plasmas*, *13*, 072904, doi:10.1063/1.2220534.

Hasegawa, H., B. U. Ö. Sonnerup, C. J. Owen, B. Klecker, G. Paschmann, A. Balogh, and H. Rème (2006), The structure of flux transfer events recovered from Cluster data, *Ann. Geophys.*, *24*, 603–618, doi:10.5194/angeo-24-603-2006.

Hau, L.-N., and B. U. Ö. Sonnerup (1999), Two-dimensional coherent structures in the magnetopause: Recovery of static equilibria from single-spacecraft data, *J. Geophys. Res.*, *104*, 6899–6917, doi:10.1029/1999JA900002.

Hu, Q., and B. Dasgupta (2005), Calculation of magnetic helicity of cylindrical flux rope, *Geophys. Res. Lett.*, *32*, L12109, doi:10.1029/2005GL023004.

Karimabadi, H., D. Krauss-Varban, and N. Omidi (1999), Magnetic structure of the reconnection layer and core field generation in plasmoids, *J. Geophys. Res.*, *104*, 12,313–12,326, doi:10.1029/1999JA900089.

Karimabadi, H., W. Daughton, and K. B. Quest (2005), Antiparallel versus component merging at the magnetopause: Current bifurcation and intermittent reconnection, *J. Geophys. Res.*, *110*, A03213, doi:10.1029/2004JA010750.

Karimabadi, H., W. Daughton, and J. Scudder (2007), Multi-scale structure of the electron diffusion region, *Geophys. Res. Lett.*, *34*, L13104, doi:10.1029/2007GL030306.

Khrabrov, A. V., and B. U. Ö. Sonnerup (1998), DeHoffmann-Teller analysis, in *Analysis Methods for Multi-Spacecraft Data*, edited by G. Paschmann and P. W. Daly, pp. 221–248, Int. Space Sci. Inst., Bern.

Klimas, A., M. Hesse, and S. Zenitani (2008), Particle-in-cell simulation of collisionless reconnection with open outflow boundaries, *Phys. Plasmas*, *15*, 082102, doi:10.1063/1.2965826.

McFadden, J. P., et al. (2008), The THEMIS ESA plasma instrument and in-flight calibration, *Space Sci. Rev.*, *141*, 277–302, doi:10.1007/s11214-008-9440-2.

Mozer, F. S., S. D. Bale, and T. D. Phan (2002), Evidence of diffusion regions at a subsolar magnetopause crossing, *Phys. Rev. Lett.*, *89*, 015002, doi:10.1103/PhysRevLett.89.015002.

Mozer, F. S., V. Angelopoulos, J. Bonnell, K. H. Glassmeier, and J. P. McFadden (2008), THEMIS observations of modified Hall fields in asymmetric magnetic field reconnection, *Geophys. Res. Lett.*, *35*, L17S04, doi:10.1029/2007GL033033.

Nakamura, M., and M. Scholer (2000), Structure of the magnetopause reconnection layer and of flux transfer events: Ion kinetic effects, *J. Geophys. Res.*, *105*, 23,179–23,191, doi:10.1029/2000JA900101.

Øieroset, M., T. D. Phan, M. Fujimoto, R. P. Lin, and R. P. Lepping (2001), In situ detection of collisionless reconnection in the Earth's magnetotail, *Nature*, *412*, 414–417, doi:10.1038/35086520.

Phan, T. D., J. F. Drake, M. A. Shay, F. S. Mozer, and J. P. Eastwood (2007), Evidence for an elongated (>60 ion skin depths) electron diffusion region during fast magnetic reconnection, *Phys. Rev. Lett.*, *99*, 255002, doi:10.1103/PhysRevLett.99.255002.

Runov, A., et al. (2003), Current sheet structure near magnetic X-line observed by Cluster, *Geophys. Res. Lett.*, *30*(11), 1579, doi:10.1029/2002GL016730.

Sibeck, D. G., and V. Angelopoulos (2008), THEMIS science objectives and mission phases, *Space Sci. Rev.*, *141*, 35–59, doi:10.1007/s11214-008-9393-5.

Sonnerup, B. U. Ö. (1979), Magnetic field reconnection, in *Solar System Plasma Physics*, edited by L. J. Lanzerotti, C. Kennel, and E. Parker, 46 pp., North-Holland, New York.

Sonnerup, B. U. Ö., and M. Guo (1996), Magnetopause transects, *Geophys. Res. Lett.*, *23*, 3679–3682, doi:10.1029/96GL03573.

Sonnerup, B. U. Ö., and M. Scheible (1998), Minimum and maximum variance analysis, in *Analysis Methods for Multi-Spacecraft Data*, edited by G. Paschmann and P. W. Daly, pp. 185–220, Int. Space Sci. Inst., Bern.

Sonnerup, B. U. Ö., H. Hasegawa, and G. Paschmann (2004), Anatomy of a flux transfer event seen by Cluster, *Geophys. Res. Lett.*, *31*, L11803, doi:10.1029/2004GL020134.

Teh, W.-L., and L.-N. Hau (2007), Triple crossings of a string of magnetic islands at duskside magnetopause encountered by AMPTE/IRM satellite on 8 August 1985, *J. Geophys. Res.*, *112*, A08207, doi:10.1029/2007JA012294.

Terasawa, T. (1983), Hall current effect on tearing mode instability, *Geophys. Res. Lett.*, *10*, 475–478, doi:10.1029/GL010i006p00475.

Vaivads, A., et al. (2004), Structure of the magnetic reconnection diffusion region from four-spacecraft observations, *Phys. Rev. Lett.*, *93*, 105001, doi:10.1103/PhysRevLett.93.105001.

V. Angelopoulos, IGPP, University of California, Los Angeles, CA 90095, USA.

J. W. Bonnell and J. P. McFadden, Space Science Laboratory, University of California, 7 Gauss Way, Berkeley, CA 94720, USA.

R. Ergun, S. Eriksson, and W.-L. Teh, Laboratory for Atmospheric and Space Physics, University of Colorado at Boulder, 1234 Innovation Dr., Boulder, CO 80303-7814, USA. (teh@lasp.colorado.edu)

K.-H. Glassmeier, Institute for Geophysics and Extraterrestrial Physics, Technical University of Braunschweig, Mendelssohnstr. 3, D-38106 Braunschweig, Germany.

B. U. Ö. Sonnerup, Thayer School of Engineering, Dartmouth College, 8000 Cummings Hall, Hanover, NH 03755-8000, USA.